LAWRENCE
LIVERMORE
NATIONAL
LABORATORY

On the Effect of Local Grain-Boundary Chemistry on the Macroscopic Mechanical Properties of a High Purity Y_2O_3-Al_2O_3-Containing Silicon Nitride Ceramic: Role of Oxygen

A. Ziegler, J.M. McNaney, M. J. Hoffmann and R. O. Ritchie

November 29, 2004

2004 MRS Fall Meeting
Boston, Massachusetts
November 29 - Dec 3 2004

On the Effect of Local Grain-Boundary Chemistry on the Macroscopic Mechanical Properties of a High Purity Y_2O_3-Al_2O_3-Containing Silicon Nitride Ceramic: Role of Oxygen

A. Ziegler[1,2], J.M. McNaney[2], M. J. Hoffmann[3] and R. O. Ritchie[4]

[1]Materials Science Division, Lawrence Berkeley National Laboratory, Berkeley, CA 94720, USA
[2]Materials Science and Technology Division, Lawrence Livermore National Laboratory, Livermore, CA 94551, USA
[3]Institut für Keramik im Maschinenbau, Universität Karlsruhe, D-76131 Karlsruhe, Germany
[4]Materials Sciences Division, Lawrence Berkeley National Laboratory and Department of Materials Science and Engineering, University of California, Berkeley, CA 94720, USA

ABSTRACT

The effects of grain-boundary chemistry on the mechanical properties were investigated on high-purity silicon nitride ceramics, specifically involving the role of oxygen. Varying the grain-boundary oxygen content, by control of oxidizing heat treatments and sintering additives, was found to result in a transition in fracture mechanism from transgranular to intergranular fracture, with an associated increase in fracture toughness. This phenomenon is correlated to an oxygen-induced change in grain-boundary chemistry that appears to affect fracture by "weakening" the interface, facilitating debonding and crack advance along the boundaries, and consequently toughening by grain bridging. It is concluded that if the oxygen content in the thin grain-boundary films exceeds a lower limit, which is ~0.87 equiv% oxygen content, then the interfacial structure and bonding characteristics favor intergranular debonding during crack propagation; otherwise, transgranular fracture ensues.

INTRODUCTION

Advanced ceramics are leading candidates to operate as structural components at high temperatures. The properties of silicon nitride ceramics are strongly influenced by microstructure and the chemical composition of the grain-boundary phase. Indeed, during processing the grain boundary is the key microstructural feature that dictates the mechanical properties. Grain boundaries in most silicon nitrides have a typical width of 1-5 nm. This equilibrium size is considered to be a function of chemical composition [1-9] rather than the amount of additive. Processing parameters such as sintering temperature, time and pressure, appear to have little effect on grain boundary thickness. The additives tend to segregate along boundaries and accumulate at the triple junctions [10,11]. Oxygen also accumulates at the boundaries, and is assumed to have a marked effect (possibly more significant than that of other sintering additives) on the mechanical properties [12,13]. Post-sintering heat treatments have invariably been found to improve the strength, creep and toughness properties of Si_3N_4 ceramics [14-20]; sound explanations as to why this happens have been generally inconclusive, in part due to the complexity of the oxidation/devitrification processes that occur during such heat treatments.

In this work, we examine two highly pure Si_3N_4 ceramics, containing Y_2O_3 and Al_2O_3 as additives, and specifically investigate the change in fracture mechanism and crack path, which is critical to defining the mechanical properties, in terms of the effect of (*i*) post-sintering heat treatments and (*ii*) slight variations in grain-boundary composition. Our approach is to focus on the role of *local* grain-boundary chemistry and its relation to crack propagation and *macroscopic* mechanical properties.

EXPERIMENTAL PROCEDURES

To minimize complications from inadvertently introduced impurities, the Si_3N_4 ceramics in the present study were uniquely fabricated without glass encapsulation, resulting in a very pure material with highly controlled amounts of sintering additives [21]. Two different Si_3N_4 compositions were examined, containing Y_2O_3 and Al_2O_3 as sintering additives and are designated as (2/0/1) and (2/0/0) by the nominal amount and type of sintering additive ($Y_2O_3/SiO_2/Al_2O_3$). Although not intentionally added, SiO_2 is an inherent component of the ceramic body, since the starting Si_3N_4 powder particles are invariably covered by a fine SiO_2 layer. The resulting microstructures of both compositions consisted of almost exclusively β-Si_3N_4 in both acicular-shaped and equiaxed grains. In addition to the as-sintered material, a set of samples of the same batch was subjected to a post-sintering heat treatment of varying duration (25, 50, 100 and 200 h) at 1400ºC in air. The average grain size and aspect ratios before and after heat treatment are listed in Table I.

Fracture toughness was measured using indentation techniques [22], the toughness being evaluated by inducing crack formation under a standard Vickers indenter using 5, 7, 10, 12 and 15 kg loads. By determining the toughness over a range of indentation loads, i.e., over a range of crack sizes, an estimate of the resistance-curve (R-curve) behavior was obtained.

Table I. Average Grain Sizes and Aspect Ratios.

Composition	ave. grain size [μm]		aspect ratio	
	a.s.	h.t.	a.s.	h.t.
(2/0/1)	2	2	8	8.1
(2/0/0)	4.1	3.9	8.3	8.2

Energy dispersive x-ray emission spectroscopy (EDX) was carried out on thin transmission electron microscopy (TEM) samples to discern the distribution of chemical elements along and across the boundaries. The EDX probe diameter could be focused to a 1.2 nm small spot to detect the signal emanating from a 1–5 nm thin grain-boundary film, whose adjacent matrix grain was oriented edge-on, mostly along [0001]. EDX spectra were collected by (*i*) line scans across the thin grain boundaries and (*ii*) spectra covering an area of 20 x 20 nm from approximately the center of the triple junctions. Scanning electron microscopy (SEM) of the fracture surfaces was performed using a JEOL 6300 scanning electron microscope.

RESULTS AND DISCUSSION

Except for grain-boundary chemistry, the microstructures of the initial as-sintered, (2/0/1) and (2/0/0) compositions differ only in grain size, whereas the grain aspect ratio is the same. Following the oxidizing heat treatments, the morphology of these microstructures appeared unchanged; there was no additional grain growth, no microstructural coarsening and no change in aspect ratio. Moreover, few triple points crystallized and many amorphous triple points remained, even after 200 h at 1400°C in both (2/0/1) and (2/0/0) compositions (Fig. 1). These images show how the amount of grain-boundary phase is distributed among triple points and thin two-grain grain boundaries; the triple points have a larger capacity than the thin films to incorporate this secondary phase.

During oxidation the diffusion paths in Si_3N_4 are primarily the grain boundaries, since at high temperatures the thin amorphous intergranular films tend to become viscous and facilitate diffusion. The formation of surface crystals in these same sample compositions [23] clearly indicates that Y and Al, and O, are diffusing through the material, which presumably allows for those elements to move to energetically more favorable atomic locations along the grain boundaries, associated with a different chemical bonding state.

The results of the indentation fracture toughness measurements are presented in Fig. 2, showing how toughness is significantly affected by the grain boundary chemistry. In the as-sintered
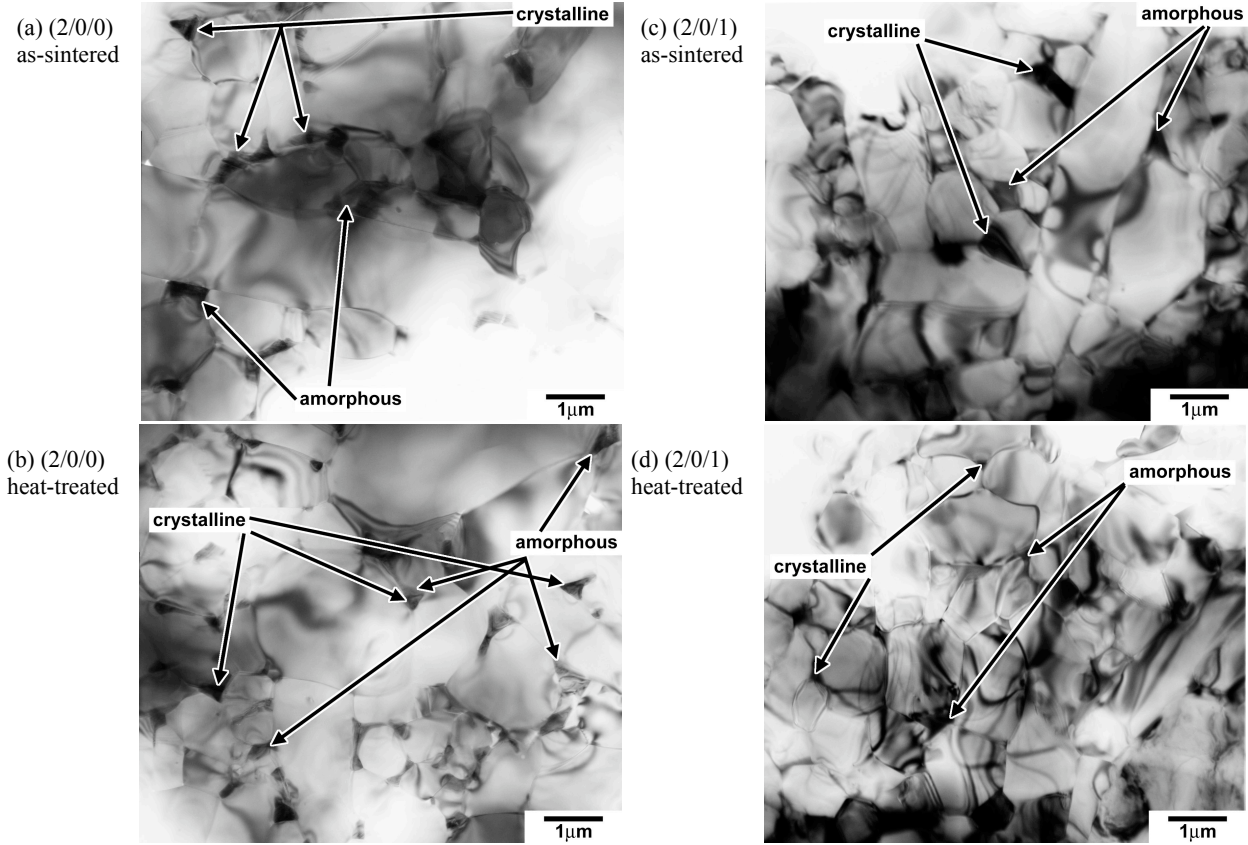
Figure 1. TEM images of the microstructure of both material compositions in their as-sintered and 200h heat-treated states respectively: (a,b) (2/0/0) and (c,d) (2/0/1). The arrows indicate crystalline and amorphous triple points.

state, the (2/0/1) material clearly shows rising *R*-curve behavior (increasing toughness with increasing crack length). Conversely, the (2/0/0) material shows no change in toughness with crack extension. However, with heat treatment, these marked differences gradually disappear, as the (2/0/0) material undergoes a marked change in fracture behavior that completely changes the shape of its *R*-curve and results in a ~180% increase in toughness. Indeed, after 200 h at 1400°C, the (2/0/0) material exhibits rising *R*-curve behavior and a fracture toughness comparable to that of the (2/0/1) material. In contrast, the evolution of the (2/0/1)

Figure 2. Indentation fracture toughness values for both material compositions in their as-sintered and the heat-treated states.

material with heat treatment is less dramatic, with only a maximum ~15% increase in toughness and no change in shape of the *R*-curve.

Fractography of the indented and subsequently fractured samples are presented in Figs. 3. They reveal that the as-sintered (2/0/0) material exhibits a brittle transgranular fracture surface
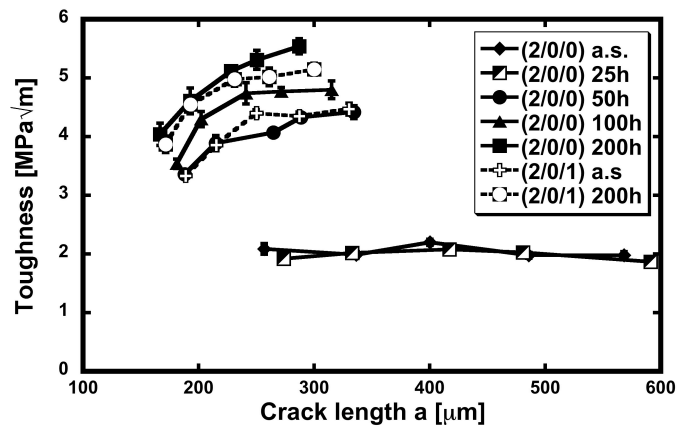
5

with no features of grain pull-out and interlocking grains that are typical of many toughened ceramic materials. After heat treatment, the (2/0/0) composition shows a distinct change in fracture mode, from largely transgranular to largely intergranular. In contrast, fracture in the (2/0/1) material remains predominantly intergranular before and after heat treatment.
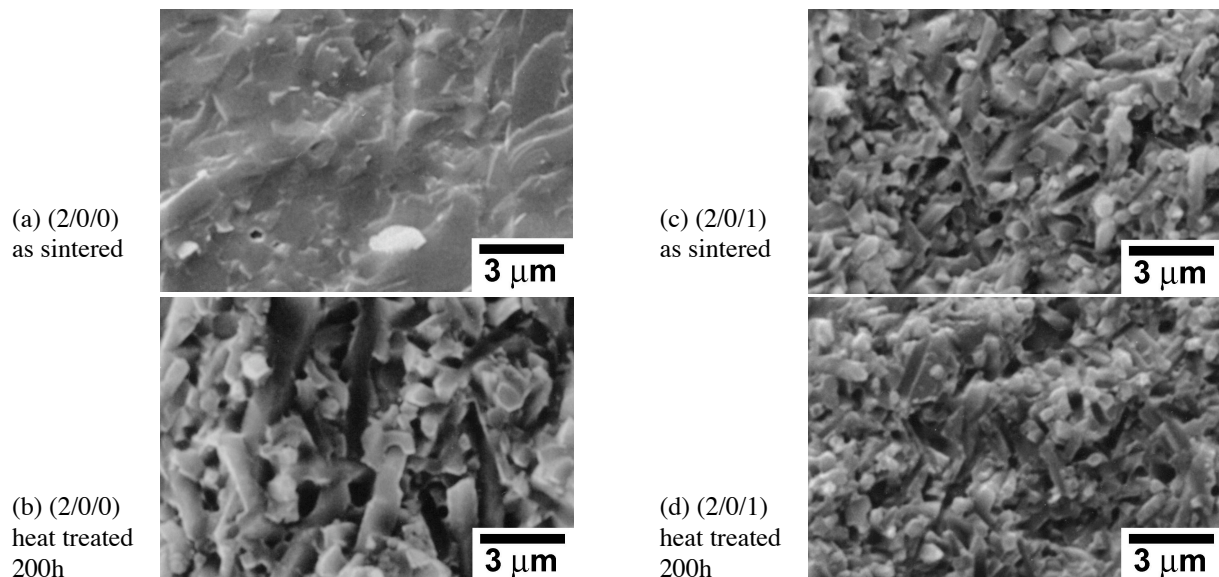

(a) (2/0/0) as sintered

3 μm

(c) (2/0/1) as sintered

3 μm

(b) (2/0/0) heat treated 200h

3 μm

(d) (2/0/1) heat treated 200h

3 μm

Figure 3. Fracture surfaces of the as-sintered and heat-treated material compositions (a,b) (2/0/0) and (c,d) (2/0/1).

The intergranular crack paths are consistent with toughening in the crack wake via crack bridging from interlocking grains which act to shield the crack tip from the applied far-field load [22,24,25]. Since the bridging is a function of crack size, this is also consistent with the observed *R*-curve behavior in Fig, 2. Irrespective of microstructural parameters such as grain size and aspect ratio, crack-bridging mechanisms in monolithic ceramics can only be active if the crack path is intergranular. The nature of the crack path is therefore a central issue, which depends strongly on how the grain-boundary chemistry determines the grain-matrix debonding characteristics.

Our hypothesis is that the observed change in fracture mechanism is associated with structural transformations in the grain-boundary phase that incorporate O, N and the sintering-additive cations, or with the relocation of these ions. With the heat-treated materials, it can be assumed that O is the major element that diffuses inward while Y, Al and N diffuse outward. Here, changes in the chemical balance and atom rearrangement are expected to only occur locally as the diffusion distances along the boundaries for these elements at 1400°C are only a few hundred micrometers. Consequently, since the possible variation in bonding is limited, we can assume that relocation of elements is more important than the inward or outward diffusion from the entire sample. Our focus is on the short-range relocation of oxygen, yttrium and aluminum, using EDX to analyze the elemental composition of the thin grain boundaries as they evolve during the heat treatment.

The results of the EDX line scans across the thin grain boundaries and the area scans on the the triple points are presented in Fig. 4, showing the evolution of the chemical composition in the grain-boundaries and triple points. It is apparent from these results that in the Al-free material (2/0/0), yttrium tends to diffuse away from the thin grain boundaries, while the amount of oxygen increases between the grains. In the Al-containing material (2/0/1), similar observations can be made:the amount of oxygen increases along the thin grain boundaries while the amount of Y and Al decreases. A corresponding EDX trend line obtained for the amorphous and crystalline triple

points show only marginal changes in their chemical composition. The notion that the triple points and the thin grain boundaries are interconnected and thus their respective transformations and chemical balances influence each other can therefore only be examined by analyzing the changes in chemistry in the thin grain boundaries.
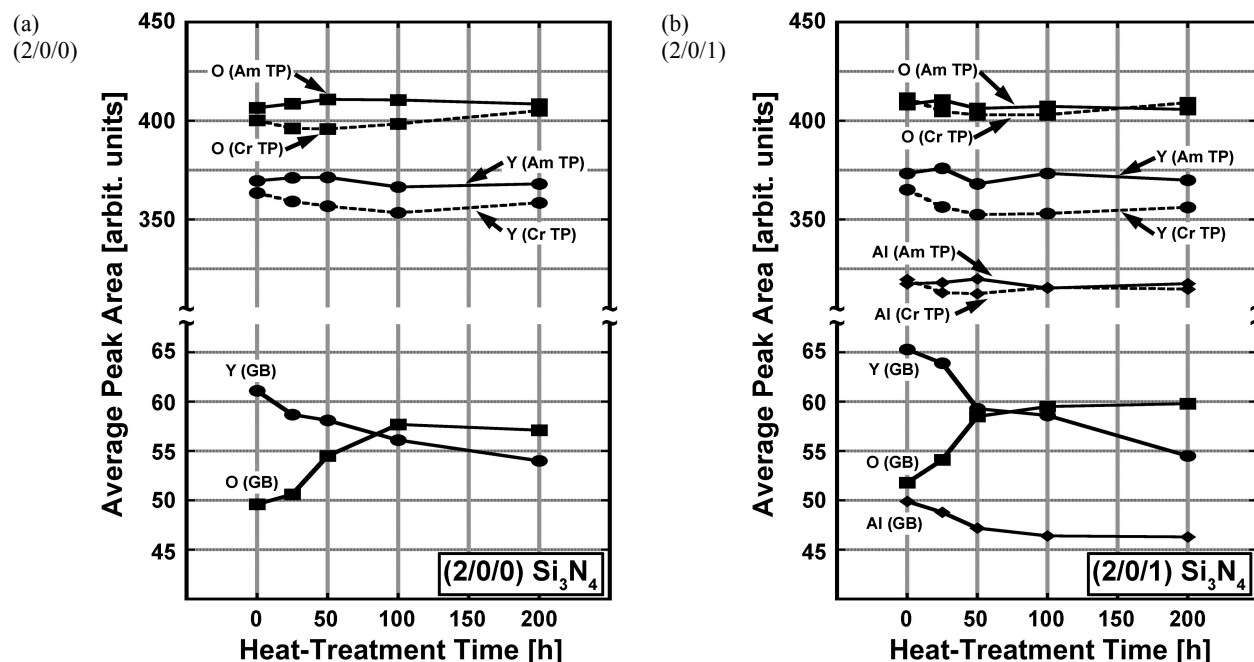
Figure 4. EDX line scans showing the evolution of the chemical composition of the grain boundaries and triple points, (a) (2/0/0) and (b) (2/0/1).

Considering the dramatic change in fracture mode in the (2/0/0) material, the immediate question is, whether there is a limit in grain-boundary oxygen content that results in the observed transition from transgranular to intergranular fracture. We have performed a qualitative analysis of the distribution and the relative volume of grain-boundary phase versus triple point(and consequently oxygen content). A critical assumption is that O is located only in, and is homogeneously distributed along, the grain-boundary phase. To determine the relative volume fraction the areas covered by the triple

Table II.   **Statistical Microstructural Parameters**

		relative area TP/GB	GB EDX signal [areal cps]	increase in GB EDX signal [%]	GB oxygen content [eq%]
(2/0/0)	a.s	3.08	49.6	--	0.79
	25h	2.93	50.6	2.02	0.81
	50h	3.03	54.5	9.88	0.87
	100h	3.16	57.7	16.33	0.92
	200h	3.01	57.1	15.12	0.91
		3.04 +/- 0.08			
(2/0/1)	a.s	2.86	51.8	--	1.04
	25h	2.84	54.1	4.44	1.09
	50h	2.91	58.5	12.93	1.17
	100h	2.97	59.5	14.86	1.19
	200h	2.90	59.8	15.44	1.20
		2.89 +/- 0.05			

TP = triple point, GB = grain boundary

points and by the boundaries were estimated from low-magnification images of the microstructure. It can be seen that the volume ratio of triple points to thin grain boundaries is approximately three, Table II. Combining this relative con-tent with the corresponding increase in EDX signals mea-sured on the thin grain boundaries can yield estimates of how much oxygen is located in the thin films. Accordingly, after 50 h at 1400°C, the EDX signal for the (2/0/0) material has increased by 9.88% and the oxygen content along the thin

7

films has increased to 0.87 equiv%. Although this is just a small increase, it is apparent that it is sufficient to locally change the bonding characteristics to such degree that it causes a fracture mode transition from transgranular to intergranular affecting so the mechanical properties at the macroscopic scale. In contrast, the (2/0/1) composition does not experience this change in fracture mode because its thin grain-boundary oxygen content is already above this critical limit in the as-sintered condition.

CONCLUSIONS

The present study has examined the effects of grain-boundary chemistry on the mechanical properties of two highly pure silicon nitride ceramics. The local oxygen content along the thin grain boundaries was increased by post-sintering heat treatment at 1400°C, resulting in a change in fracture mode from transgranular to intergranular with a concomitant dramatic increase in fracture toughness by ~180%. Such a marked change was found to be associated with the incorporation of oxygen into the thin grain boundaries as revealed by EDX analyses. It is concluded that if a lower limit of ~0.87 equiv% oxygen-content in the grain boundary phase is exceeded, then the interfacial structure and bonding characteristics change in favor of intergranular debonding during crack propagation; otherwise transgranular fracture occurs.

ACKNOWLEDGEMENTS

REFERENCES

[1]   Clarke, D.R., *J. Am. Ceram. Soc.*, **70** 15 (1987).
[2]   Kleebe, H. J., Bruley, J. and Rühle, M., *J. Eur. Ceram. Soc.*, **14**, 1 (1994).
[3]   Gu, H., Pan, X., Cannon, R. M. and Rühle, M., *J. Am. Ceram. Soc.*, **81** 3125 (1998).
[4]   Kleebe, H.J., Cinibulk, M.K., Cannon, R.M. and Rühle, M., *J. Am. Ceram. Soc.*, **76** 1969 (1993).
[5]   Clarke, D. R., Shaw, T. M., Philipse, A. P. and Horn R. G., *J. Am. Ceram. Soc.*, **76** 1201 (1993).
[6]   Kleebe, H. J., Hoffmann, M. J. and Rühle, M., *Z. Metallkd.*, **83** 610 (1992).
[7]   Tanaka, I., Kleebe, H. J., Cinibulk, M. K., Bruley, J., Clarke, D. R. and Rühle, M., *J. Am. Ceram. Soc.*, **77** 911 (1994).
[8]   Pan, X., Gu, H., van Weeren, R., Danforth, S. C., Cannon, R. M. and Rühle, M., *J. Am. Ceram. Soc.*, **79** 2313 (1996).
[9]   Wang, C. M., Pan, X., Hoffmann, M. J., Cannon, R. M. and Rühle, M., *J. Am. Ceram. Soc.*, **79** 788 (1996).
[10]   Cinibulk, M. K., Thomas, G. and Johnson, S. M., *J. Am. Ceram. Soc.*, **75** 2037 (1992).
[11]   Clarke, D.R., Zaluzec, N.J. and Carpenter, R.W., *J. Am. Ceram. Soc.*, **64** 601 (1981).
[12]   Becher, P. F., Sun, E. Y., Hsueh, C. H., Alexander, K. B., Hwang, S. L. Waters, S. B. and Westmoreland, C. G., *Acta Mat.*, **44** 3881 (1996).

[13]   Sun, E. Y., Alexander, K. B., Becher, P. F. and Hwang, S. L., *J. Am. Ceram. Soc.*, **79** 2626 (1996).
[14]   Cinibulk, M.K., Thomas, G. and Johnson, S.M., *J. Am. Ceram. Soc.*, **73** 1606 (1990).
[15]   Bonnell, D.A., Tien, T.Y. and Rühle, M., *J. Am. Ceram. Soc.*, **70** 460 (1987).
[16]   Bodur, C. T., Szabo, D. V. and Kromp, K., *J. Mat. Sci.*, **28** 2089 (1993).
[17]   Cinibulk, M.K. and Kleebe, H.J., *J. Mat. Sci.*, **28** 5775 (1993).
[18]   Lange, F.F., Davis, B.I. and Graham, H.C., *J. Am. Ceram. Soc.*, **66** C98 (1983).
[19]   Lange, F.F, Davis, B.I. and Metcalf, M.G., *J. Mat. Sci.*, **18** 1497 (1983).
[20]   Klemm, H. and Pezzotti, G., *J. Am. Ceram. Soc.*, **77** 553 (1994).
[21]   Hoffmann, M. J., Geyer, A., Oberacker, R., *J. Euro. Ceram. Soc.*, **19**, 2359 (1999).
[22]   Lawn, B. R., *Fracture of Brittle Solids*, 2nd ed., Cambridge Univ. Press (1993).
[23]   Ziegler A., McNaney, J. M., Hoffmann, M. J., Ritchie, R. O., *J. Am. Ceram. Soc*. in review
[24]   Ritchie, R.O., *Mater. Sci. Eng.,* **A103** 15 (1988).
[25]   Becher, P. F., *J. Am. Ceram. Soc.*, **74** 255 (1991).